

# Influence of Processing on the Microstructural Development and Flexure Strength of $\text{Al}_2\text{O}_3/\text{SiC}$ Nanocomposites

C. E. Borsa,<sup>a,\*</sup> N. M. R Jones,<sup>a</sup> R. J. Brook<sup>a</sup> & R. I. Todd<sup>b</sup>

<sup>a</sup>Department of Materials, Oxford University, Oxford, OX1 3PH, UK

<sup>b</sup>Manchester Materials Science Centre, University of Manchester and UMIST, Grosvenor St, Manchester, M1 7HS, UK

(Received 16 April 1996; revised version received 16 August 1996; accepted 29 September 1996)

## Abstract

*Alumina/10 wt% SiC nanocomposites were prepared by using a number of processing techniques, in order to produce different microstructures while keeping a uniform distribution of the SiC particles in the alumina matrix. Basically, this study used three techniques, i.e. mechanical mixture of powders, the use of an inorganic precursor for alumina precipitated onto SiC particles and the use of different polymeric precursors for SiC precipitated on alumina particles. Hot pressing at 1700°C was necessary to produce fully dense nanocomposites. The alumina precursor route produced the smallest matrix grain size and the SiC precursor route produced the smallest reinforcement particle size. Despite the differences in microstructure between the nanocomposites, the flexure strength remained the same, and no distinct improvement over the monolithic alumina was observed. The fracture mode, however, changed from intergranular to transgranular with the presence of the SiC particles.*

© 1997 Elsevier Science Limited. All rights reserved.

## 1 Introduction

Engineering ceramics have great potential to replace and improve upon high-temperature metals in many demanding applications. Ceramics possess intrinsic properties which make them attractive for applications where low density, high stiffness, high hardness, chemical inertness and good high-temperature properties are required,

such as heat exchangers, heat engines and metal shaping equipment.<sup>1</sup>

Despite these promising characteristics the widespread commercial use of structural ceramics has yet to come about. Monolithic ceramics suffer from defects which are intimately related to the specific processing methods used in manufacturing. Such defects, be they pores, cracks, organic and inorganic inclusions, etc., can severely limit the mechanical strength of the ceramic material, leading to catastrophic failure.<sup>2</sup>

Attempts to improve the strength and the strength variability of advanced ceramics have, therefore, been the focus of attention of ceramic researchers over the past three decades. As a result, a number of different approaches have been proposed in this area.<sup>3</sup> Of these, the use of second-phase reinforcements (e.g. whiskers, particulates and platelets) is one of the most prominent. It attempts to create microstructures with improved fracture resistance which will also lead to an increase in flexure strength. The size of these reinforcing phases is usually several micrometres or more.

Improved strength has also been obtained by the addition of nano-size second phases as reported by Niihara and his colleagues<sup>4</sup> for alumina reinforced by 200 nm SiC particles. In this case, however, the strength improvement of 300% achieved was greater than normally obtained for the use of second-phase reinforcements. The toughness improved less dramatically, by 50% over monolithic alumina. Other works in this system have also showed some strengthening of this material although the level of improvement was lower.<sup>5,6</sup> A number of possible explanations for these properties have been advanced, but none has gained great acceptance.<sup>4–6</sup>

A reasonable way of making progress is to change the microstructural variables of the material

\*To whom correspondence should be addressed at: Universidade Federal de São Carlos, Departamento de Engenharia de Materiais, Via Washington Luiz, Km 235-São Carlos-SP 13565-915 Brazil.

systematically, such as matrix grain size, reinforcement particle size, etc., while keeping an homogeneous distribution of the second phase. However, this is frequently very difficult to achieve because of the preparation techniques normally used to produce the nanocomposite, i.e. mechanical mixture of commercial  $\text{Al}_2\text{O}_3$  and SiC powders followed by hot pressing. Under these conditions, the microstructure obtained has an effectively predetermined alumina grain size, dictated by the pinning force of the SiC particles, which are randomly distributed throughout the matrix.<sup>7</sup> In order to be able to modify the microstructure of the material, different preparation techniques must be used.

The aim of this work, was to prepare  $\text{Al}_2\text{O}_3/\text{SiC}$  nanocomposites having different microstructural features, such as matrix grain size and shape, and SiC particle size, and so to provide a better way of understanding the active mechanisms in this material. Three different preparation techniques were used, namely, the mechanical mixture of powders, use of an inorganic precursor for the alumina phase, and use of a polymeric precursor for the SiC. Additionally, the influence of these changes on the flexure strength of the different materials is reported and compared with results from monolithic alumina. The results showed that the microstructures obtained were easily altered by the alternative preparation techniques, but the strength results were not sensitive to these variations.

## 2 Experimental Procedure

### 2.1 Preparation of the nanocomposite powder

Homogeneous mixtures of  $\text{Al}_2\text{O}_3/\text{SiC}$  nanocomposite powders were prepared using three different routes as described below.

#### 2.1.1 Mechanical mixture powders

In this route, commercial nano-sized  $\text{Al}_2\text{O}_3$  powder (APK53, Sumitomo, mean particle size  $0.2\ \mu\text{m}$ ) was mechanically mixed with commercial SiC powder (UF45, Lonza, mean particle size  $0.2\ \mu\text{m}$ ) or with a chemically vapour deposited SiC powder, prepared in-house. Details of the CVD experiment can be found elsewhere.<sup>8</sup> The preparation of both nanocomposite materials and the monolithic alumina (doped with 0.2% MgO), followed the same steps. In order to improve the dispersion and to break up the hard agglomerates of the SiC powder, it was ultrasonically dispersed in distilled water before mixing with the desired amount of  $\text{Al}_2\text{O}_3$ . Small additions of a dispersant (Dispex A40, Allied Colloids) were used to deflocculate the  $\text{Al}_2\text{O}_3$ . The powders were then attrition

milled for 1.5 h (weight ratio of water to powder = 1) using magnesia-stabilised zirconia media, flocculated by adding HCl and finally dried for 24 h at  $80^\circ\text{C}$  in a plastic tray. The flocculation of the matrix powder was found to prevent the segregation and agglomeration of the SiC nano-particles.

#### 2.1.2 Alumina precursor

In this route, SiC powder was coated with a controlled layer of an  $\text{Al}_2\text{O}_3$  precursor formed by a heterogeneous precipitation reaction. The method was used on a route for coating SiC whiskers.<sup>9</sup> Urea ( $\text{CO}(\text{NH}_2)_2$ , Aldrich) and hydrated aluminium nitrate (AN) ( $\text{Al}_2(\text{NO}_3)_3 \cdot 9\text{H}_2\text{O}$ , Aldrich) were used as the reagents in the reaction. An aqueous solution was prepared containing 12 g/litre of urea and 0.3 M of AN. This was slowly heated in a spherical flask connected to a condenser, to reduce the loss of water, over a period of 2 h to the process temperature  $85^\circ\text{C}$ . The solution was magnetically stirred and the changes in the pH were continuously measured by a pH meter. This condition was maintained until the pH increased from 1.5 to 4. At this time a pre-heated aqueous dispersion of 5 g/litre of SiC was added to the solution (using a 1:1 ratio) and aged for 24 h under vigorous stirring. Under this condition, the precipitation of a complex of aluminium hydroxide (CAH) occurred, coating the SiC particles. Following the coating, the suspension was cooled to room temperature and allowed to settle, after which the supernatant was discarded and the remaining slurry washed with deionised water and dried at  $80^\circ\text{C}$  for 24 h. The resulting powder was calcined at high temperatures ( $1150^\circ\text{C}$ ) in Ar for 2 h. During this treatment, CAH was converted to a porous alumina. The powder was then ball milled in propan-2-ol for 3 h using alumina balls and dried at  $80^\circ\text{C}$  for 24 h.

#### 2.1.3 SiC precursor

For this route two different polymers were used as source of SiC, a polysilazane (Polyvinylmethylsilylhydrazine, PV, Elf Atochem) and a polysilastyrene polymer (PSS 400, Nippon Soda). Both materials were prepared following similar steps. Initially the polymer was dissolved in toluene (10 g: 100 ml) and then mixed with the alumina powder. The dispersion was then ball milled for 3 h using alumina balls and dried under low vacuum. The blend was broken up using a pestle and mortar and crosslinked at  $400^\circ\text{C}$  for 3 h, then pyrolysed at  $1000\text{--}1500^\circ\text{C}$  for 2 h. All heat treatments were done in an Ar/1%  $\text{H}_2$  atmosphere using  $5^\circ\text{C}/\text{h}$  for the heating rate in the crosslinking step and  $5^\circ\text{C}/\text{min}$  for the pyrolysis step. A boat with graphite powder was placed inside the furnace

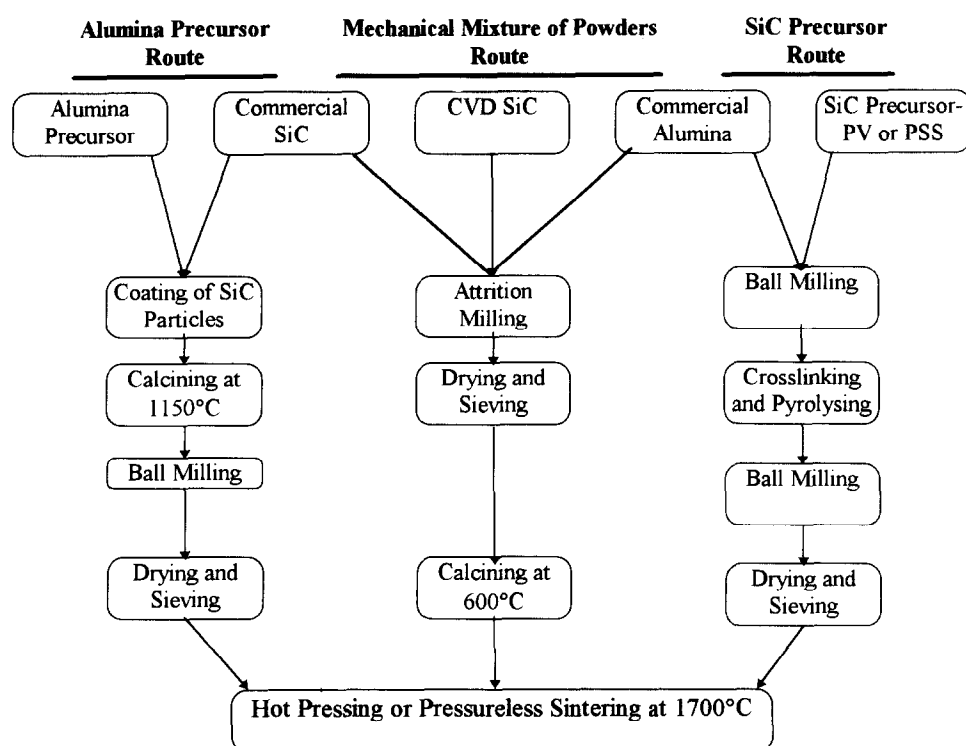


Fig. 1. Schematic diagram illustrating the preparation steps used in the different processing routes.

during the pyrolysis stage in an attempt to reduce the oxidation reaction of the polymer. The powder was ball milled in propan-2-ol for 3 h using alumina balls and dried at 80°C for 24 h.

Figure 1 shows a schematic diagram illustrating the preparation steps for the different processing routes.

## 2.2 Densification of the materials

The dried nanocomposite powder produced by the different preparation routes was broken up using a pestle and mortar and passed through a 180- $\mu\text{m}$  sieve. For pressureless sintering experiments, the powders were uniaxially pressed with the aid of a binder (PVA 2 wt% of the  $\text{Al}_2\text{O}_3$  content) at 170 MPa and calcined in air at 600°C (apart from the organic route samples) for 5 h. Sintering was carried out in a closed end recrystallised  $\text{Al}_2\text{O}_3$  tube furnace, heated by molybdenum disilicide elements, under an Ar-1%  $\text{H}_2$  atmosphere. The pellets were surrounded by SiC powder and heated at 1700°C for the nanocomposite and between 1400 and 1550°C for pure  $\text{Al}_2\text{O}_3$  for 2 h using a heating rate of 5°C/min. In addition, calcined powders were uniaxially hot-pressed in a graphite die (1 h/25 MPa/Ar) at 1700°C for the nanocomposites and at 1400°C for the monolithic  $\text{Al}_2\text{O}_3$ .

## 2.3 Characterisation techniques

Sintered densities were measured using the Archimedes method; X-ray diffraction was used to

check for the presence of extra phases arising from oxidation or reaction. For microstructural observation, the samples were polished using diamond paste to a 3- $\mu\text{m}$  finish. The  $\text{Al}_2\text{O}_3$  and the nanocomposite were thermally etched between 1350 and 1450°C/1h using a closed end  $\text{Al}_2\text{O}_3$  tube furnace in either vacuum ( $10^{-5}$  MPa) or Ar/1%  $\text{H}_2$ . The etched sections were carbon coated and examined using SEM (JEOL 6300). The average grain size was measured by the linear intercept method. TEM (JEOL 200 CX) was used to check the particle size and the morphology of the powders used, and the distribution of nano-particles inside the grains. Thin samples were prepared by dimpling the samples down to 60  $\mu\text{m}$  and by ion beam thinning until a hole was produced in the material. X-ray mapping was used to identify the elemental composition of the materials.

The four-point bend test was used to evaluate the strength of the hot-pressed materials. The samples (25 mm  $\times$  2.5 mm  $\times$  2.0 mm), were produced as follows. First the discs were diamond ground flat to a thickness of 2.1 mm. Then the beams were cut using a diamond saw, after which the tensile face and the two sides of the beam were polished by removing 100  $\mu\text{m}$  of material with 3- $\mu\text{m}$  diamond in order to eliminate any residual stresses generated by the machining step. The tensile edges were bevelled to reduce the effect of edge cracks, by waxing the bars (two each time) in a 90° grooved brass and polishing for 25 min with a 3- $\mu\text{m}$  diamond. The tests were performed in

an Instron machine using a speed of 0.5 mm/min and a load cell of 500 kg. The strength of the alumina precursor material could not be determined owing to the small amount of material produced.

### 3 Results and Discussion

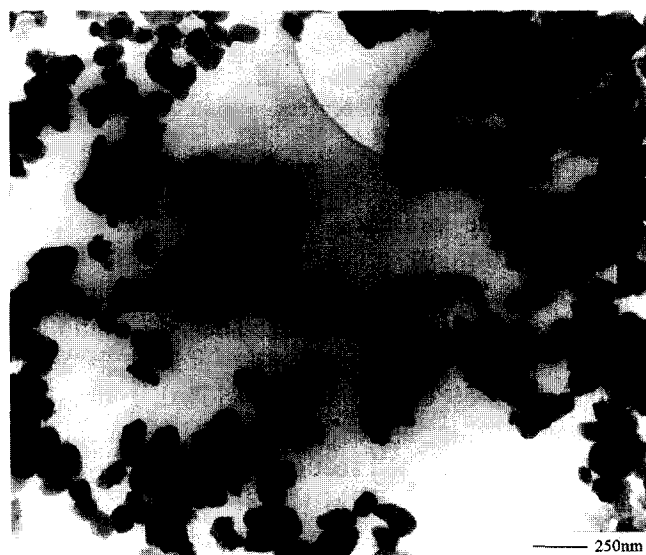
#### 3.1 Powder characterisation

Figure 2 shows TEM micrographs of the commercial  $\text{Al}_2\text{O}_3$  and SiC powders used in the mechanical mixture of powders route. The observed average particle size of the SiC powder (Fig. 2(b)) is in agreement with the recommended size for its use as a reinforcement phase in nanocomposite materials, i.e. <300 nm.<sup>4</sup> However, a vigorous mixing step in well-controlled conditions (where both powders are stabilised in the medium) is necessary

to achieve an homogeneous material by this processing route.

For samples prepared by the alumina precursor route, Fig. 3 shows a TEM micrograph of commercial SiC particles coated by a porous phase formed by the precipitation reaction of an aluminium precursor. The coated phase transformed to  $\alpha$ -alumina upon heating at 1150°C. The elongated aspect ratio of the coating phase was reduced after ball milling.

Figure 4 shows a TEM micrograph of the alumina powder coated by nano-sized SiC particles prepared by the PSS-SiC precursor route. The nano-sized SiC was obtained by the controlled thermal decomposition of a polymer at the temperature of 1500°C. This temperature is necessary to crystallise the SiC particles, which can, however, lead to the formation of sintered structures



(a)



(b)

Fig. 2. TEM micrographs of the commercial powders used in the mechanical mixture route: (a) alumina, and (b) SiC.

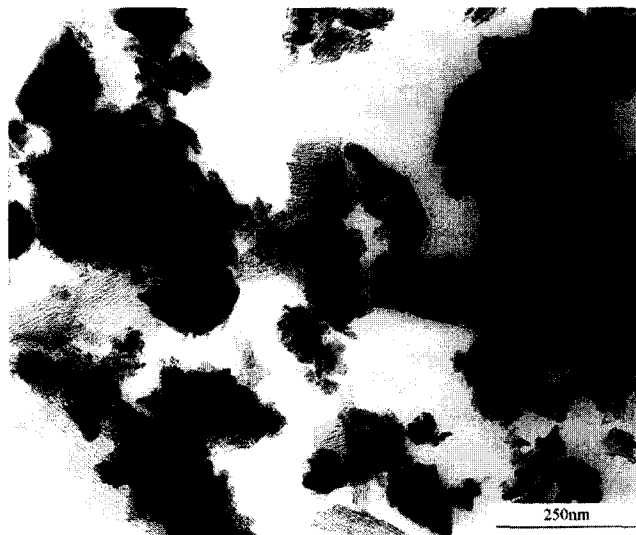


Fig. 3. TEM micrograph of the coated SiC particles obtained by the precipitation reaction in the alumina precursor route.

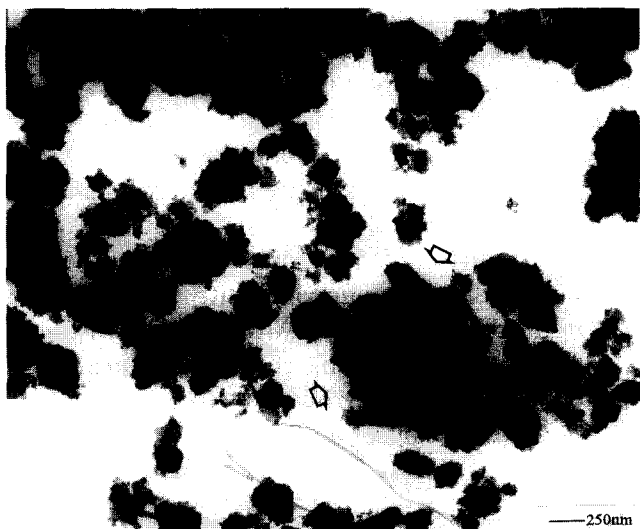


Fig. 4. TEM micrograph of alumina powder coated by 10–20 nm SiC particles obtained by the controlled thermal decomposition of the PSS polymer at 1500°C.

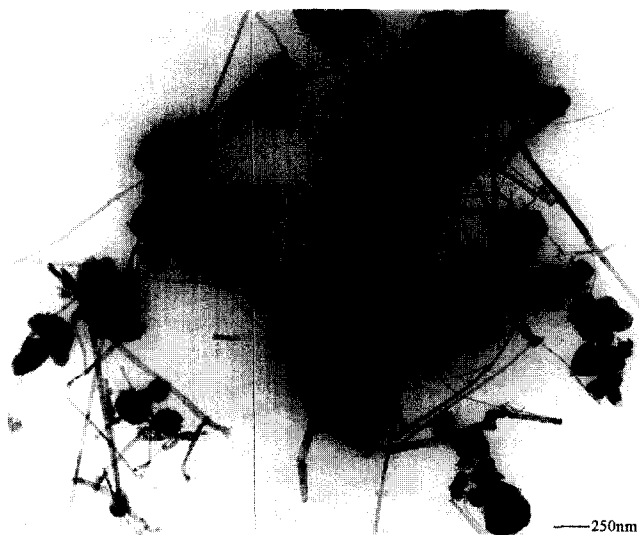


Fig. 5. TEM micrograph of the SiC whisker network mixed with the alumina particles formed by thermal decomposition of the PV polymer at 1500°C.

as shown by the arrows of Fig. 4. An efficient milling stage is then needed to break down these agglomerates.

Regarding the PV-SiC powders, the heat treatment at high temperatures formed a network of whiskers instead of particles as shown in Fig. 5. This can be explained by considering the higher presence of oxygen in the as-received PV (5.4 wt%). In these conditions, SiC whiskers can be synthesised from a known reaction between Si atoms transferred as  $\text{SiO}_{(\text{g})}$  and carbon atoms as  $\text{CH}_4$  and  $\text{C}_2\text{H}_2$  by the vapour-liquid-solid (VLS) process.<sup>10</sup> Therefore, lower pyrolysis temperatures had to be used for this material, i.e. 1300°C, which avoided whiskers formation, but was not enough to eliminate undesirable substances which will react with the alumina at high temperatures forming a range of second phases. This fact prevented the use of hot pressing for this polymer. However, pressureless sintering experiments could be carried out if the material was pyrolysed as a pressed pellet covered with SiC powder bed rather than as loose powder. In these conditions, the material was well protected from the furnace atmosphere and VLS reactions which can lead to the formation of whiskers were avoided.

### 3.2 Densification behaviour

Pressureless sintering of these powders did not lead to full densification, which is desirable for meaningful evaluation of the strength of the nanocomposites. The reasons for this, already discussed in previous works,<sup>6,7</sup> are related to the presence of the nano-sized SiC particles. For the polymer-precursor route, however, the excess of carbon present in the pyrolysed nanocomposite powders could further reduce the densification of

the materials, by the formation of gaseous products ( $\text{SiO}$  or  $\text{CO}$ ) during the sintering process. Furthermore, PV contains nitrogen and should form  $\text{Si}_3\text{N}_4$  in addition to SiC, which reacts with carbon at temperatures higher than 1440°C releasing  $\text{N}_2$ . The presence of these gases may also introduce voids in the material to the detriment of the mechanical properties.

Hot pressing at 1700°C was then used for most of the routes, except the PV-SiC precursor route, as discussed in the last section. Pressureless sintering at 1700°C was used in this case and a density of 92% of the theoretical value was achieved.

### 3.3 Microstructure analysis

Figure 6 shows TEM micrographs of nanocomposite materials prepared by the different processing routes. Significant differences between their microstructures can be observed, with variations in matrix grain size and morphology, and particle size and distribution. Table 1 presents a summary of the microstructural characteristics for each material.

Nanocomposite materials processed by the mechanical mixture of powders showed a variety of behaviours. Whereas the samples prepared from commercial powders contained an homogeneous dispersion of the SiC particles mainly inside the alumina grains (Fig. 6(a)), samples prepared by using the CVD-SiC powder displayed coarsened SiC particles, poorly dispersed and situated mainly at the grain boundaries of the alumina (Fig. 6(b)). This difference in microstructure probably derived from the difficulties of dispersing the very fine SiC powder produced by the CVD reaction which remained agglomerated throughout the processing.

Samples prepared using SiC precursors (Figs 6(c) and (d)) contained very small SiC particles, as expected from the in-situ chemical formation of the particles during the decomposition of the polymer.<sup>11</sup> The PSS-derived nanocomposite, however, had a heterogeneous dispersion of the SiC particles with matrix grain size varying from 0.5  $\mu\text{m}$  to 10  $\mu\text{m}$ , in contrast to the PV-derived materials where an homogeneous distribution of SiC was achieved in an equiaxed alumina matrix. The better homogeneity and smaller particle size of PV- compared to PSS-derived materials can be explained based on the differences in the dispersion of these polymers during the homogenisation step. PSS, a neutral polymer, does not provide steric deflocculation for the alumina powder in organic media. This results in a heterogeneous mixture of the ingredients, which remains throughout the process, leading to abnormal grain growth of the matrix in regions where there are no particles, and growth of the SiC particles where their

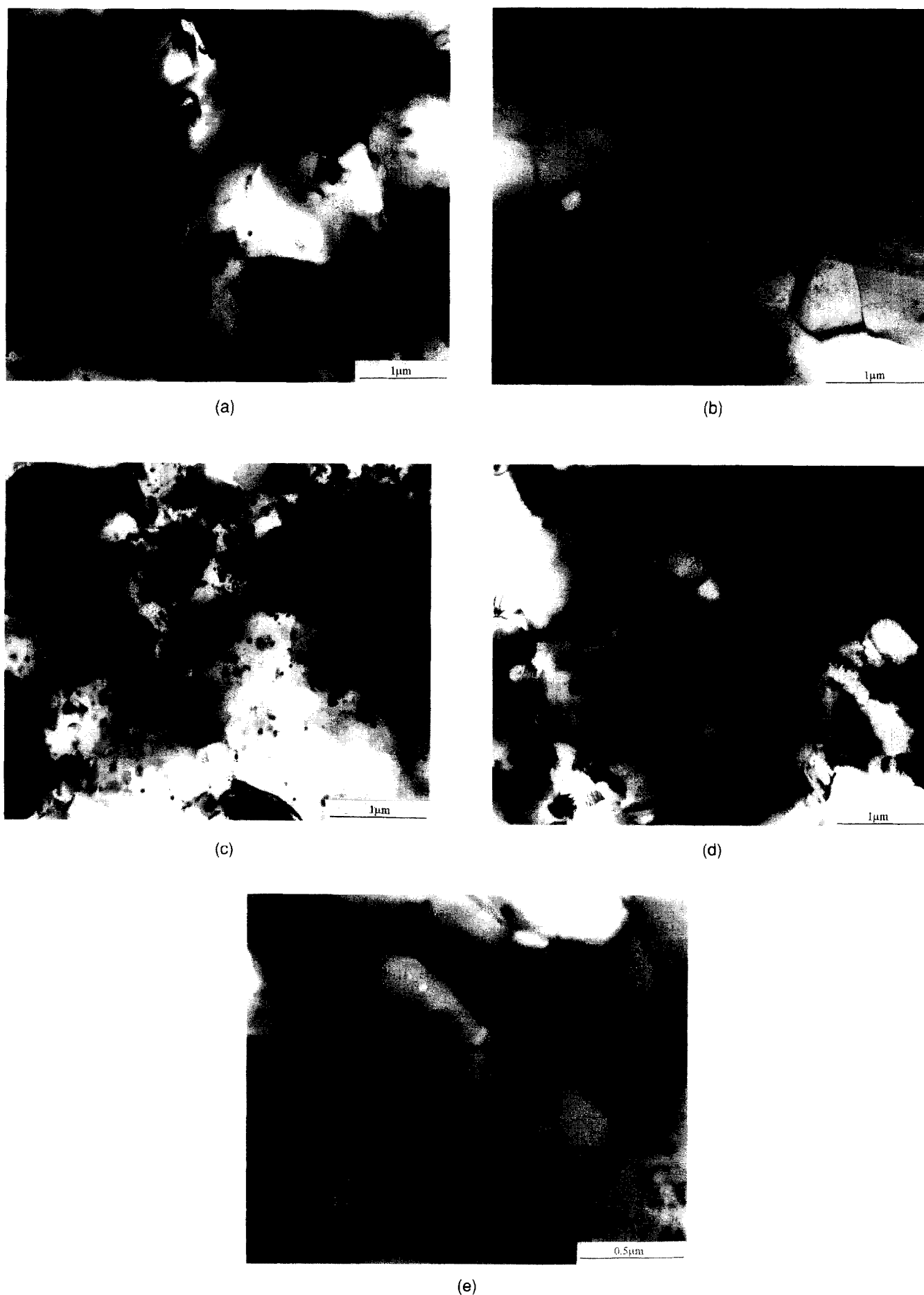


**Fig. 6.** TEM micrograph of dense nanocomposite materials prepared by different processing routes: (a) mechanical mixture of powders, commercial; (b) mechanical mixture of powders, CVD SiC; (c) PSS-SiC precursor; (d) PV-SiC precursor; and (e) alumina precursor.

**Table 1.** Summary of the microstructural characteristics for each material

<i>Preparation route</i>	<i>Range of SiC particle size</i>	<i>Average grain size and morphology of the <math>\text{Al}_2\text{O}_3</math> matrix</i>	<i>Predominant location of SiC particles</i>
Mixture of powders, commercial	50–200 nm	2.5 $\mu\text{m}$ , equiaxial	Inside the grains
Mixture of powders, CVD-SiC	200–500 nm	3.2 $\mu\text{m}$ , equiaxial	At the grain boundaries
$\text{Al}_2\text{O}_3$ precursor	50–200 nm	1.1 $\mu\text{m}$ , elongated	Both inside and at the grain boundaries
PSS-SiC precursor	30–200 nm	1.5 $\mu\text{m}$ ., equiaxial with bimodal grain size distribution	Inside the grains
PV-SiC precursor	10–70 nm	4.2 $\mu\text{m}$ , equiaxial	Inside the grains

concentration is higher. In contrast, PV is a polar polymer, so the precursor mixes well with the alumina and the opposite behaviour is observed.

For nanocomposites prepared by the alumina precursor route (Fig. 6(e)), the most significant feature is the very small grain size of the alumina matrix and its elongated morphology. The SiC particles are well dispersed and are situated both on the alumina grain boundaries and within the grains. The reason for this distinctive behaviour of morphology of the alumina grains is not known in detail, but since the alumina had a different origin from the powders used in the other specimens there is no reason to expect them to give the same final microstructure.

X-ray diffraction carried out on all materials confirmed the presence of only  $\text{Al}_2\text{O}_3$  and SiC phases.

### 3.4 Strength results

Table 2 presents the four-point bend strengths of the different groups of materials. Despite the significant differences among the microstructures shown in Fig. 6, the strength results did not vary greatly. Compared to the monolithic alumina of similar grain size (2.6  $\mu\text{m}$ ), the only specimens to show a measurable strength improvement were those prepared using the PSS-SiC precursor, and the increase was only 10%. Moreover, the group which gave the highest average value for strength (PSS-derived material) is the one which has the most heterogeneous microstructure. This is in contrast with most literature data,<sup>4,5,12</sup> which show

gains in strength varying from 30 to 300%, although these values are quoted for 5 vol% nanocomposite materials. It seems that factors other than the microstructure controlled the maximum strength of the materials in this work, such as processing defects common to both materials or surface damage caused by machining. The quality of the surface finishing can have a strong effect in this particular system. Porteman *et al.*<sup>13</sup> found that in tests where no strength improvement over monolithic alumina was obtained initially, an improvement of 30% was achieved if a more gentle machining of the surface was carried out. No processing defects (pores, agglomerates, etc.) could be identified at the fracture origin in the present work, so it is likely that the critical flaws were caused by machining in this case.

Analysis of the fracture surface of the nanocomposite materials showed that the fracture passes through the alumina grains as opposed to the monolithic alumina which fractures along its grain boundaries. This happened for all nanocomposites despite the differences in microstructure, which suggests that this change in path stems directly from the presence of SiC particles, irrespective of their size or position in the alumina matrix.

## 4 Conclusions

1. Alumina/SiC nanocomposites with different microstructures were prepared using a variety of processing routes, viz. mechanical mixture of powders, use of an alumina precursor and use of a SiC precursor.
2. Hot pressing at 1700°C was necessary to produce fully dense nanocomposites. Processing routes involving the in-situ phase formation produced the smallest size for that phase. The alumina precursor route produced the smallest average matrix grain size (1.1  $\mu\text{m}$ ) and the SiC precursor route produced the

**Table 2.** Four-point bend strength for the materials prepared by different routes

<i>Material</i>	<i>Flexure strength (MPa)</i>
Monolithic alumina	626 $\pm$ 32
Mixture of powders, commercial	638 $\pm$ 12
Mixture of powders, CVD SiC	625 $\pm$ 28
PSS-SiC precursor	688 $\pm$ 17

smallest average reinforcement particle size (50 nm).

3. The fracture mode changed from intergranular in monolithic alumina to transgranular with the presence of the SiC particles. This happened for all nanocomposites despite the differences in the microstructures, which indicates the strong effect on fracture of the presence of SiC particles compared to other variables.
4. The microstructural variation among the nanocomposites produced little difference in strength. Little or no difference in strength improvement over the monolithic alumina was observed, despite the change in fracture mode. This was attributed to the critical flaws being produced by machining damage rather than being directly related to the microstructure.

### Acknowledgements

The authors are grateful to CNPq (Brazil), the EU (Brite/Euram contract BRE CT92 0358) and the SERC for the financial support, and to Oxford University for the provision of laboratory facilities.

### References

1. Taguchi, M., Application of high-technology ceramic in Japanese automobiles. *Adv. Ceram. Mater.*, **3**(4) (1987) 1759–1762.
2. Danforth, S. C. In *Proceedings of the International Symposium on Advances in Processing of Ceramic and Metal Matrix Composites*, ed. H. Mostaghaci. Halifax, 1989, p. 107.
3. Evans, A. G., Perspective on the development of high-toughness ceramics. *J. Am. Ceram. Soc.*, **73**(2) (1990) 187–206.
4. Niihara, K. & Nakahira, A., Structural ceramic nanocomposites by sintering method: Roles of nano-size particles. *Ceramics: Toward the 21st Century*, Ceram. Soc. of Japan, 1991, pp. 404–417.
5. Zhao, J., Stearns, L. C., Harmer, M. P., Chan, H. M., Miller, G. A. & Cook, R. C., Mechanical behaviour of  $\text{Al}_2\text{O}_3/\text{SiC}$  nanocomposites. *J. Am. Ceram. Soc.*, **76**(2) (1993) 503–510.
6. Borsa, C. E., Jiao S., Todd, R. I. & Brook, R. J., Processing and properties of  $\text{Al}_2\text{O}_3/\text{SiC}$  nanocomposites. *J. Microscopy*, **177**(3) (1995) 305–312.
7. Stearns, C. L., Zhao, J. & Harmer, M. P., Processing and microstructure development in  $\text{Al}_2\text{O}_3/\text{SiC}$  nanocomposites. *J. Eur. Ceram. Soc.*, **10** (1992) 473–477.
8. Jones, N. M. R., DPhil Thesis, Oxford University, Oxford, 1995.
9. Kalponek, D. & De Jonghe, L. C., Particulate composites from coated powder. *J. Eur. Ceram. Soc.*, **7** (1991) 345–351.
10. Saito, M., Nagashima, S. & Kato, A., Crystal growth of SiC whisker from the  $\text{SiO}(\text{g})\text{-CO}$  system. *J. Mater. Sci. Lett.*, **11** (1992) 373–376.
11. Riedel, R., Strecker, K. & Petzow, G., In-situ polysilane-derived silicon carbide particulates dispersed in silicon nitride composites. *J. Am. Ceram. Soc.*, **72**(11) (1989) 2071–2077.
12. Wohlfrohm, H. In *Ceramic Processing Science and Technology, Ceramic Transactions*, vol. 51, ed. G. Messing et al. American Ceramic Society, Ohio, 1995, 648. pp.
13. Porteman, M., Development of nanocomposite materials with enhanced mechanical properties. *Brite-Euram Project*, BRE CT921358, Project Report, Nov. 1994.